Dietary Feeding of Silibinin Inhibits Prostate Tumor Growth and Progression in Transgenic Adenocarcinoma of the Mouse Prostate Model

Komal Raina,[1] Marie-José Blouin,[4] Rana P. Singh,[1,5] Noreen Majeed,[4] Gagan Deep,[1] Leyon Varghese,[1] L. Michael Glodé,[2,3] Norman M. Greenberg,[6] David Hwang,[7] Pinchas Cohen,[7] Michael N. Pollak,[4] and Rajesh Agarwal[1,3]

[1]Department of Pharmaceutical Sciences, School of Pharmacy, [2]Department of Medicine, and [3]University of Colorado Cancer Center, University of Colorado Health Sciences Center, Denver, Colorado; [4]Lady Davis Institute for Medical Research, Jewish General Hospital and Department of Oncology, McGill University, Montreal, Quebec, Canada; [5]Cancer Biology Laboratory, School of Life Sciences, Jawaharlal Nehru University, New Delhi, India; [6]Clinical Research Division, Fred Hutchinson Cancer Research Center, Seattle, Washington; and [7]Mattel Children's Hospital, University of California at Los Angeles, Los Angeles, California

Abstract

Herein, for the first time, we evaluated the chemopreventive efficacy of dietary silibinin against prostate cancer (PCa) growth and progression in transgenic adenocarcinoma of the mouse prostate (TRAMP) mice from two different genetic backgrounds [C57BL/6 (TRAMP) × FVB; C57BL/6 (TRAMP) × C57BL/6]. At 4 weeks of age, mice were fed control or 0.1% to 1% silibinin–supplemented diets until 23 to 24 weeks of age. Silibinin-fed groups had a lower tumor grade and higher incidence of prostatic intraepithelial neoplasia (PIN) at the expense of a strong decrease in adenocarcinoma incidence. Prostate tissue showed a 47% ($P < 0.001$) decrease in proliferating cell nuclear antigen (PCNA)–positive cells and an ~7-fold ($P < 0.001$) increase in apoptotic cells at the highest silibinin dose. As potential mechanisms of silibinin efficacy, an ~50% ($P < 0.05$) decrease in insulin-like growth factor (IGF) receptor type Iβ and an ~13-fold ($P < 0.001$) increase in IGF-binding protein 3 (IGFBP-3) protein levels were also observed. These changes were specific to tumors as they were not reflected in circulating IGF-IGFBP-3 system. Additionally, silibinin decreased protein expression of cyclin-dependent kinases (Cdk) by more than 90% ($P < 0.001$) with a concomitant increase in Cdk inhibitors, Cip1/p21 and Kip1/p27 ($P < 0.05$, for both). A dose-dependent decrease was also observed in cyclin B1, cyclin E, and cyclin A protein levels by silibinin. Together, these findings suggest that oral silibinin blocks PCa growth and progression at PIN stage in TRAMP mice via modulation of tumor IGF-IGFBP-3 axis and cell cycle regulation, and therefore it has practical and translational potential in suppressing growth and neoplastic conversion of PIN to PCa in humans.

Introduction

Prostate cancer (PCa) is the most common malignancy in American men, and second only to lung cancer in deaths (1). With time, PCa progresses to a hormone-refractory stage, rendering antiandrogen therapy ineffective (2, 3). However, onset of preclinical PCa may occur in men as early as 30 years of age and takes considerable time for progression to detectable malignancy, and, accordingly, a considerable window of time may allow for various prevention strategies to be used (3). Recently, there have been considerable activities directed toward identification of dietary or nondietary naturally occurring chemical agents for both prevention and intervention of PCa (4–6). One such agent is silibinin, which has shown promising chemopreventive and anticancer effects in various *in vitro* and *in vivo* studies (7).

Silibinin is a flavonolignan isolated from milk thistle (*Silybum marianum*) seeds. Silibinin and its cruder form, silymarin, are well known for their hepatoprotective activity and used clinically and as dietary supplements against liver toxicity for decades (8). Both silibinin and silymarin inhibit growth of many cancers of epithelial origin, including PCa (3, 7, 9). Silibinin possesses strong anticancer efficacy against both androgen-dependent and androgen-independent PCa, wherein it inhibits cell growth and induces cell cycle arrest in human PCa LNCaP, PC-3, and DU145 cells (10–13). Additionally, growth inhibitory and proapoptotic effects of silibinin are observed in mouse tumorigenic TRAMP-C1 cells.[8] Mechanistically, silibinin induces differentiation morphology; reduces prostate specific antigen level; and induces cell cycle arrest accompanied by an increase in cyclin-dependent kinase (Cdk) inhibitors, inhibition of Cdk activity, decrease in phosphorylation of retinoblastoma (Rb) and related proteins, and their increased interaction with E2F family of transcription factors in cell culture (3). Silibinin also inhibits *in vivo* growth of DU145 xenograft in nude mice, which is mediated, in part, by an induction of insulin-like growth factor–binding protein 3 (IGFBP-3; ref. 14). However, the chemopreventive efficacy of silibinin in a PCa model other than xenograft and the *in vivo* effect of silibinin on Cdk-cyclin-Cdk inhibitor axis and IGF type I receptor β (IGF-IRβ) signaling and their significance have not been studied in any existing animal models of PCa.

Here, for the first time, we evaluated the chemopreventive efficacy of dietary silibinin feeding against PCa growth and progression and associated molecular alterations in transgenic adenocarcinoma of the mouse prostate (TRAMP) model, which was developed in C57BL/6 mice using minimal rat probasin promoter (PB) to drive the expression of SV40 early genes (T/t; Tag)

specifically in prostatic epithelium (15, 16). The transgene is hormonally regulated, expressed at sexual maturity, and induces spontaneous neoplastic epithelial transformation (17). SV40 large T antigen abrogates p53 and Rb function; as a result, TRAMP male mice develop spontaneous progressive stages of prostatic disease with time from early lesions of prostatic intraepithelial neoplasia (PIN) to late-stage metastatic adenocarcinoma and closely mimic the progressive forms of human prostatic carcinoma (15, 18–20). Therefore, our present findings of chemopreventive efficacy of silibinin and associated mechanisms in TRAMP model could have potential clinical significance.

Materials and Methods

Animals, treatment, and necropsy. TRAMP mice from two different genetic backgrounds were studied to ensure that silibinin efficacy was strain independent. Heterozygous TRAMP females, developed on a pure C57BL/6 background, were cross-bred with either nontransgenic C57BL/6 or FVB breeder males. Tail DNA was subjected to PCR-based screening assay for PB-Tag (17), and routinely obtained 4-week-old TRAMP male mice from specific genetic backgrounds were randomly distributed into control and treatment groups.

In the first experiment, C57BL/6 (TRAMP) × FVB (TRAMP/FVB) mice were fed control AIN-93M (n = 17, positive control) or 0.5% (w/w) silibinin–containing (n = 17) diet for 19 weeks. In the second experiment, C57BL/6 (TRAMP) × C57BL/6 (TRAMP/C57BL/6) mice were fed control and silibinin [0.1%, 0.5%, and 1% silibinin (w/w) in AIN-93M purified] diets for 20 weeks; there were 17, 15, 18, and 16 mice in positive control, 0.1%, 0.5%, and 1% silibinin–fed groups, respectively. As overall controls, nontransgenic mice (n = 5 mice per group) were fed control or highest silibinin dose diet for same time. All diets were prepared commercially by Dyets. Silibinin was from Sigma and its purity checked as >98% as described (21). During the study, animals were permitted free access to drinking water and food. Food consumption and animal body weight were recorded weekly, and animals were monitored daily for their general health. Animal care and treatments were in accordance with Institutional guidelines and approved protocol.

At the time of sacrifice, the animals were anesthetized by ketamine injection and then euthanized by exsanguination. Serum was separated from the collected blood and stored at −80°C. Each mouse was weighed and lower urogenital tract including bladder, seminal vesicles, and prostate was removed *en bloc*. Lower urogenital tract wet weight was recorded and prostate gland harvested and microdissected whenever possible (when a tumor obscured the boundaries of the lobes it was taken as such). In TRAMP/C57BL/6 group, one portion of dorsolateral prostate was snap frozen and stored at −80°C. Tissues were fixed overnight in 10% (v/v) phosphate-buffered formalin and processed conventionally. Sections (5 μm) of paraffin-embedded tissues were stained with H&E for routine histopathologic evaluation. At the time of necropsy, animals were also examined for gross pathology, and any evidence of edema, abnormal organ size, or appearance in nontarget organs was also noted.

Immunohistochemical analysis. Paraffin-embedded sections were deparaffinized and stained with specific primary antibody followed by 3,3′-diaminobenzidine (DAB) staining, as previously described (22). Primary antibodies used were anti-SV40 large T antigen (1:400; BD PharMingen), anti-PCNA (1:250; DAKO), anti–IGF-IRβ (1:50; Cell Signaling), and anti–IGFBP-3 (1:25; Santa Cruz Biotechnology). Biotinylated secondary antibodies used were rabbit anti-mouse immunoglobulin G (IgG; 1:200; DAKO) and goat anti-rabbit IgG (1:200; Santa Cruz Biotechnology). Apoptotic cells were identified by terminal deoxynucleotidyl transferase–mediated dUTP nick end labeling (TUNEL) staining using Dead End Colorometric TUNEL System (Promega Corp.). PCNA- and TUNEL-positive cells were quantified by counting brown-stained cells within total number of cells at 10 randomly selected fields at ×400 magnification. For IGF-IRβ and IGFBP-3, immunoreactivity (represented by intensity of brown staining) was scored as 0 (no staining), +1 (nonuniform and very weak), +2 (nonuniform and weak), +3 (uniform and moderate), and +4 (uniform and strong).

ELISA assays for mouse IGF-I, IGFBP-2, and IGFBP-3. Mouse recombinant IGF-I, IGFBP-2, and IGFBP-3 protein standards, monoclonal antibodies, and biotinylated polyclonal antibodies were from R&D Systems. Levels of murine IGF-I, IGFBP-2, and IGFBP-3 were measured using in-house enzyme-linked immunoassays as published (23). IGF-I assay has a sensitivity of 0.1 ng/mL. The intra-assay and interassay coefficients of variation were <10% in the range of 1 to 10 ng/mL. IGFBP-2 and IGFBP-3 assays have a sensitivity of 0.2 ng/mL. The intra-assay and interassay coefficients of variation were <6% and <8%, respectively, in the range of 1 to 6 ng/mL.

Immunoblot analysis. Dorsolateral prostate samples from positive control and silibinin-fed groups of mice were analyzed by immunoblotting as previously described (13). Primary antibodies were anti–IGFBP-3, anti-Cdk2, anti-Cdk4, anti-Cdk6, anti-Cdc2, anti–cyclin A, anti–cyclin B1 (Santa Cruz Biotechnology); anti–cyclin E (Ab-1), anti-Kip1/p27 (NeoMarkers); anti-Cip1/p21 (Upstate); and anti–IGF-IRβ and anti–pIGF-IR-Tyr^{1131} (Cell Signaling). Secondary antibodies were antirabbit IgG (Cell Signaling) or antimouse IgG (Amersham). Equal protein loading was confirmed by stripping and reprobing membranes with anti–β-actin primary antibody (Sigma).

Statistical and microscopic analyses. All statistical analyses were carried out with Sigma Stat software version 2.03 (Jandel Scientific), and two-sided $P < 0.05$ was considered significant. χ^2 analysis and Fisher's exact test were used to compare incidence of PIN and adenocarcinoma in positive control group versus silibinin-fed group. For other data, the difference between positive control group versus silibinin-fed group was analyzed by unpaired two-tailed Student's t test and one-way ANOVA followed by Bonferroni t test for pairwise multiple comparisons. Densitometric analysis of immunoblots (adjusted with β-actin as loading control) was done with Scion Image program (NIH). All microscopic histopathologic and immunohistochemical analyses were done with Zeiss Axioscope 2 microscope (Carl Zeiss, Inc.) and photomicrographs were captured with Carl Zeiss AxioCam MrC5 camera.

Results

Silibinin feeding reduces lower urogenital tract weight. In TRAMP/FVB mice study, dietary silibinin feeding did not show any considerable change in diet consumption and there was no considerable difference in body weight between the positive control and silibinin-fed mice during the entire treatment regimen (data not shown). At the time of necropsy, all animals were examined for gross pathology, and there was no evidence of edema, abnormal organ size, or appearance in nontarget organs. However, there was a significant difference in lower urogenital tract weight between positive control (6.78 ± 1.54 g) and silibinin-fed group (1.75 ± 0.54 g); the latter was 74% ($P < 0.01$) lower compared with positive control. When lower urogenital tract weight was normalized to body weight (Fig. 1*A*), silibinin-fed mice showed 66% ($P < 0.05$) lower urogenital tract weight compared with the positive control. In subsequent experiment with TRAMP/C57BL/6 mice assessing dose-dependent effect of silibinin feeding (0.1–1% silibinin, w/w), consistent with the first experiment, silibinin did not show any observable change in diet consumption and body weight of mice throughout the treatment (data not shown). At necropsy, silibinin decreased lower urogenital tract weight compared with the positive control group, although statistically not significant (data not shown). Silibinin-treated groups did not show any considerable decrease in the levels of SV40 T antigen in different stages of prostate tumorigenesis compared with the positive control group as observed by immunohistochemical analysis of the transgene expression (Supplementary Fig. S1). In

nontransgenic mice, silibinin did not show any change in lower urogenital tract weight (data not shown).

Silibinin feeding reduces adenocarcinoma incidence. H&E-stained sections were microscopically examined and classified based on Shappell et al. (24) with some modifications: (*a*) low-grade PIN having foci with two or more layers of atypical cells with elongated hyperchromatic nuclei and intact gland profiles; (*b*) high-grade PIN having increased epithelial stratification, foci of atypical cells fill or almost fill the lumen of the ducts, enlarged diameter of glands, distorted duct profiles, increase in nuclear pleomorphism, hyperchromatic nuclei, and cribriform structures; (*c*) well-differentiated adenocarcinoma showing invasion of basement membrane, loss of intraductal spaces, and increased quantity of small glands; (*d*) moderately differentiated adenocarcinoma showing total loss of intraductal spaces and relatively solid growth; and (*e*) poorly differentiated adenocarcinoma showing sheets of poorly differentiated cells with remnants of trapped glands.

In TRAMP/FVB mice study, histopathologic analysis of prostate followed the same trend as gross pathology showing less aggressiveness in silibinin-fed group. As shown in Fig. 1*B*, in silibinin-fed group, on average, 45 $\pm$ 8% area of prostate gland was histologically normal compared with a 29 $\pm$ 5% normal area in the positive control. Further, the area covered by PIN lesions in silibinin-fed group was 50% less than that in the positive control group, although well-differentiated area in silibinin-fed group was 36 $\pm$ 6% compared with 24 $\pm$ 5% in the positive control. There was a significant difference in the area covered by more aggressive tumors between silibinin-fed and positive control groups; silibinin-fed group had 63% (P < 0.05) less poorly differentiated area compared with the positive control. Furthermore, 15% of silibinin-fed mice had a 100% disease-free (normal) prostate whereas none in the positive control group had an absolutely normal prostate (Fig. 1*C*), and 12% of mice in the positive control group had 100% of their prostate tissue replaced by adenocarcinoma, with half of them displaying 100% poorly differentiated adenocarcinoma.

In subsequent TRAMP/C57BL/6 mice study, detailed histopathologic analysis revealed that there was a marked difference in tumor incidence between the positive control and silibinin-fed groups. As shown in Fig. 2*A*, there was a difference in PIN incidence between silibinin-fed and positive control groups. None of the mice showed low-grade PIN in control and 0.1% silibinin–fed groups; however, there was an emergence of low-grade PIN in 16% and 31%

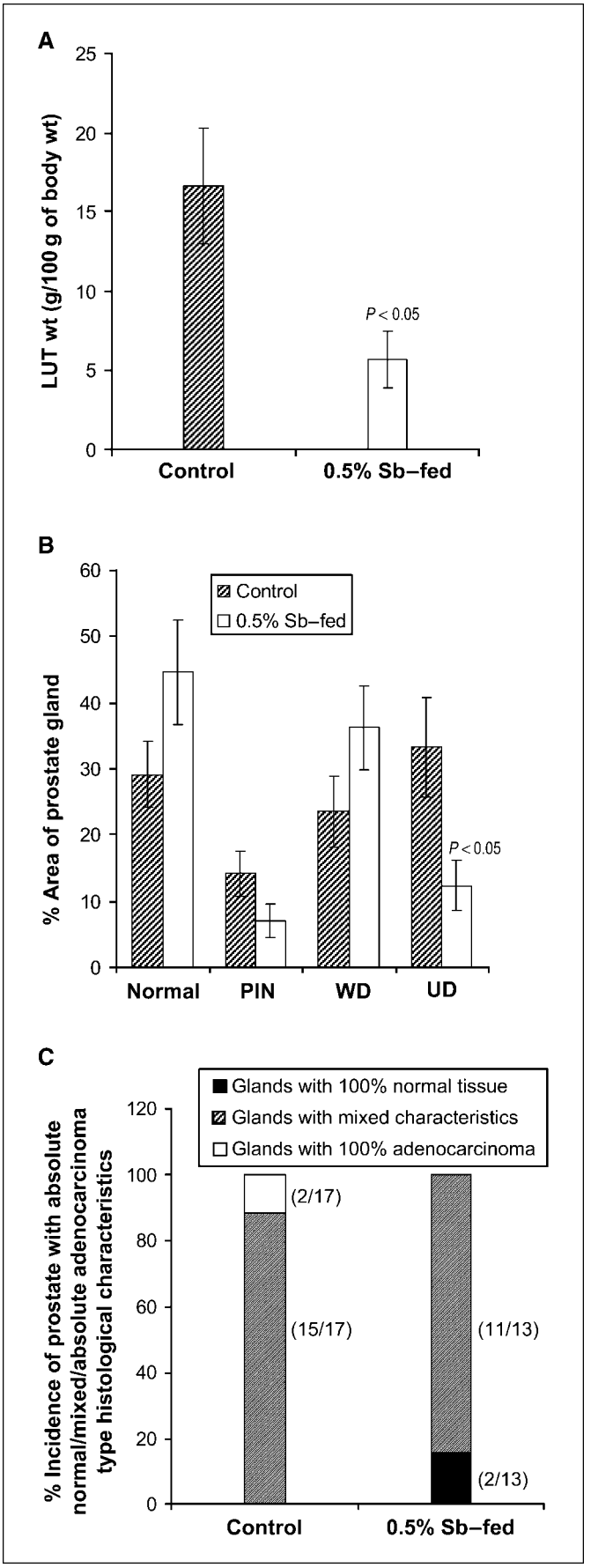

Figure 1. Inhibitory effect of silibinin diet on prostate tumorigenesis in TRAMP/FVB mice. *A,* effect of silibinin diet on the weight of the lower urogenital tract (*LUT*) organs. At the time of necropsy after 19 wk of silibinin feeding (0.5% silibinin in diet) starting from 4th week of age, each mouse was weighed and the lower urogenital tract including the bladder, seminal vesicles, and prostate was removed *en bloc* and weighed. n = 17 (positive control), n = 13 (0.5% silibinin–fed) mice per group; *bars,* SE. The statistical significance of difference between positive control and silibinin-fed groups was analyzed by unpaired two-tailed Student's t test. P < 0.05 was considered significant. *B,* percentage of area of prostate gland of positive control and silibinin-fed groups having histologically normal, PIN, well-differentiated (*WD*), and undifferentiated (*UD*; both moderately and poorly differentiated) adenocarcinoma characteristics. *Bars,* SE. The statistical significance of difference between the specific pathologic state of positive control versus silibinin-fed group was analyzed by unpaired two-tailed Student's t test. P < 0.05 was considered significant. *C,* effect of silibinin feeding on the percentage of mice having 100% disease-free (absolute normal) prostate, 100% of the prostate tissue replaced by adenocarcinoma (absolute adenocarcinoma), and mixed characteristics of the type ranging from normal, PIN, to adenocarcinoma. Values in parentheses denote actual number of animals. *Control,* positive control (TRAMP mice); *Sb,* silibinin.

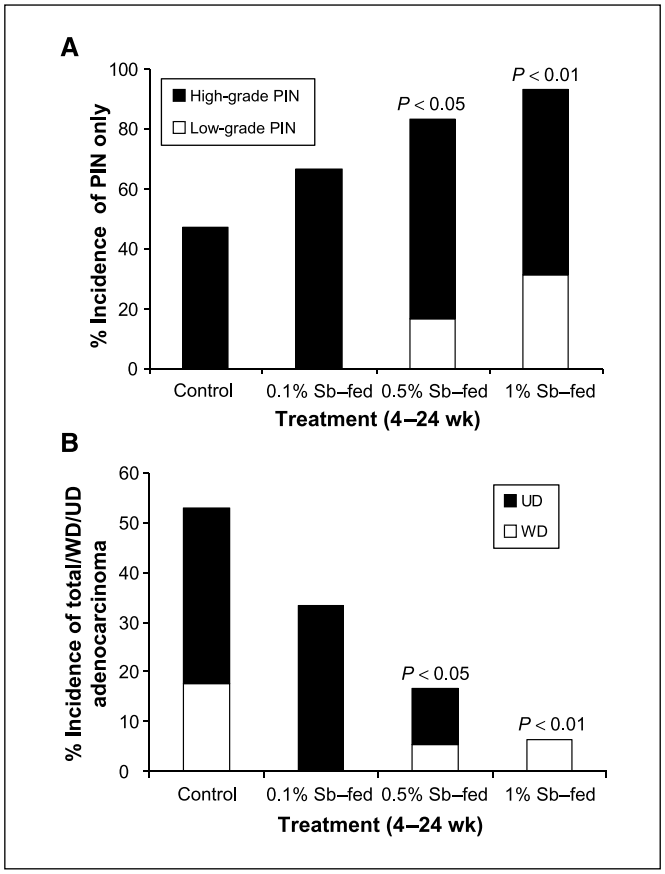

Figure 2. Silibinin feeding inhibits neoplastic progression of prostate in TRAMP/C57BL/6 mice. At the time of necropsy after 20 wk of silibinin feeding (0.1%, 0.5%, and 1% silibinin in diet) starting from 4th week of age, each mouse was weighed and the lower urogenital tract including the bladder, seminal vesicles, and prostate was removed *en bloc*. $n = 17$ (positive control), $n = 15$ (0.1% silibinin fed), $n = 18$ (0.5% silibinin fed), and $n = 16$ (1% silibinin fed) mice per group. The prostate glands were histopathologically analyzed for the different stages of the neoplastic progression. *A,* effect of silibinin feeding on the incidence of PIN lesions in TRAMP/C57BL/6 mice. *B,* effect of silibinin on the incidence of adenocarcinoma of prostate in TRAMP/C57BL/6 mice. χ^2 analysis and Fisher's exact test were used to compare incidence of PIN and adenocarcinoma in positive control versus silibinin-fed groups. $P < 0.05$ was considered significant.

of mice in 0.5% and 1% silibinin–fed groups, respectively. Similarly, high-grade PIN incidence was also noted to increase from 47% in positive control to 66%, 66%, and 62% in 0.1%, 0.5% and 1% silibinin–fed groups, respectively (Fig. 2*A*). However, there was a concomitant dose-dependent decrease in adenocarcinoma incidence in silibinin-fed groups of mice compared with the positive controls (Fig. 2*B*). There were 69% and 64% reductions in the incidence of well-differentiated tumors in 0.5% and 1% silibinin–fed group compared with the positive control mice, respectively. The incidence of undifferentiated (both moderately and poorly differentiated) tumors decreased from 35% in positive control to 33% and 11% in 0.1% and 0.5% silibinin–fed groups, respectively (Fig. 2*B*). Strikingly, none of the mice showed moderately or poorly differentiated adenocarcinoma in 1% silibinin–fed group (Fig. 2*B*). In nontransgenic mice, prostate histopathology did not show any difference in control and silibinin-fed groups (data not shown). These results suggest that silibinin feeding causes a dose-dependent decrease in the incidence of adenocarcinoma and blocks tumor progression at PIN stages.

Silibinin feeding also reduces tumor grade. Because silibinin dose-response study was conducted in TRAMP/C57BL/6 mice, we decided to restrict further analysis only to the tissues obtained from this study. As progressive pathologies of the disease are more evident and aggressive in dorsolateral prostate, further studies were conducted with a particular focus on dorsolateral prostate. To assess severity of prostatic lesions, histologic data of TRAMP/C57BL/6 mice were further analyzed for tumor grade. Tissues were graded according to the criteria by Hurwitz et al. (25), where (*a*) normal epithelium was assigned a score of 1.0; (*b*) low-grade PIN as 2.0; (*c*) high-grade PIN as 3.0; (*d*) well-differentiated adenocarcinoma as 4.0; (*e*) moderately differentiated adenocarcinoma as 5.0; and (*f*) poorly differentiated adenocarcinoma as 6.0. To generate a mean peak histologic score, the maximum histologic score for individual prostate from each mouse was used to calculate a mean for that treatment group. As shown in Fig. 3*A*, there was a significant reduction in the severity of lesions in 0.5% and 1% silibinin–fed groups. Specifically, TRAMP mice fed with 1% silibinin had a significantly lower tumor grade (mean peak score, 2.7; $P < 0.001$) than the positive control group (mean peak score, 4.0). The 0.5% silibinin–fed group also had a significantly lower tumor grade (mean peak score, 3.2; $P < 0.05$) than the positive control, whereas the 0.1% silibinin–fed group had only a slightly lower tumor grade (mean peak score, 3.9). The photomicrographs, representative of mean peak histologic score of a treatment group, are shown in Fig. 3*B*. These results convincingly suggest that, in addition to reducing adenocarcinoma incidence, silibinin feeding decreases the severity of prostatic lesions in a dose-dependent manner.

Silibinin feeding reduces proliferation index but increases apoptosis. To assess the *in vivo* effect of silibinin feeding on proliferation index in the dorsolateral prostate, tissue samples from TRAMP/C57BL/6 mice were analyzed by PCNA immunostaining. Qualitative microscopic examination of PCNA-stained sections showed a substantial decrease in PCNA-positive cells in silibinin-fed groups compared with the positive control (Fig. 4*A*). Quantification of PCNA staining showed 47 $\pm$ 5%, 36 $\pm$ 7%, and 31 $\pm$ 4% PCNA-positive cells in 0.1%, 0.5%, and 1% silibinin–fed groups of mice compared with 58 $\pm$ 2% in the positive control (Fig. 4*A*), accounting for a decrease in proliferation indices by 19%, 38% ($P < 0.01$), and 47% ($P < 0.001$), respectively. These results suggest an *in vivo* antiproliferative effect of silibinin during tumor growth and progression in dorsolateral prostate of TRAMP mice.

Regarding *in vivo* apoptotic response of silibinin feeding on prostate tumorigenesis in TRAMP/C57BL/6 mice, microscopic examination of tissue sections showed an increased number of TUNEL-positive cells in silibinin-fed groups (Fig. 4*B*). The numbers of TUNEL-positive apoptotic cells were 13 $\pm$ 0.7%, 18 $\pm$ 1%, and 26 $\pm$ 4% in 0.1%, 0.5%, and 1% silibinin–fed groups of mice, respectively, compared with 4 $\pm$ 0.3% in the positive controls, accounting for an $\sim$7-fold ($P < 0.001$) increase in apoptotic cells by highest silibinin dose. This finding suggests that proapoptotic effect could be another potential mechanism underlying chemopreventive effect of silibinin on prostate tumorigenesis in TRAMP model.

Silibinin impairs IGF-I signaling pathway. Recently, we showed that silibinin has an antiproliferative effect against PC-3 cells *in vitro* and induces IGFBP-3 secretion to inhibit IGF-I signaling (13), and that it inhibits *in vivo* growth of DU145 xenograft with a concomitant increase in tumor IGFBP-3 and its secretion in mouse plasma (14, 22). These findings prompted us to assess whether dietary silibinin had an effect on IGF-IR signaling

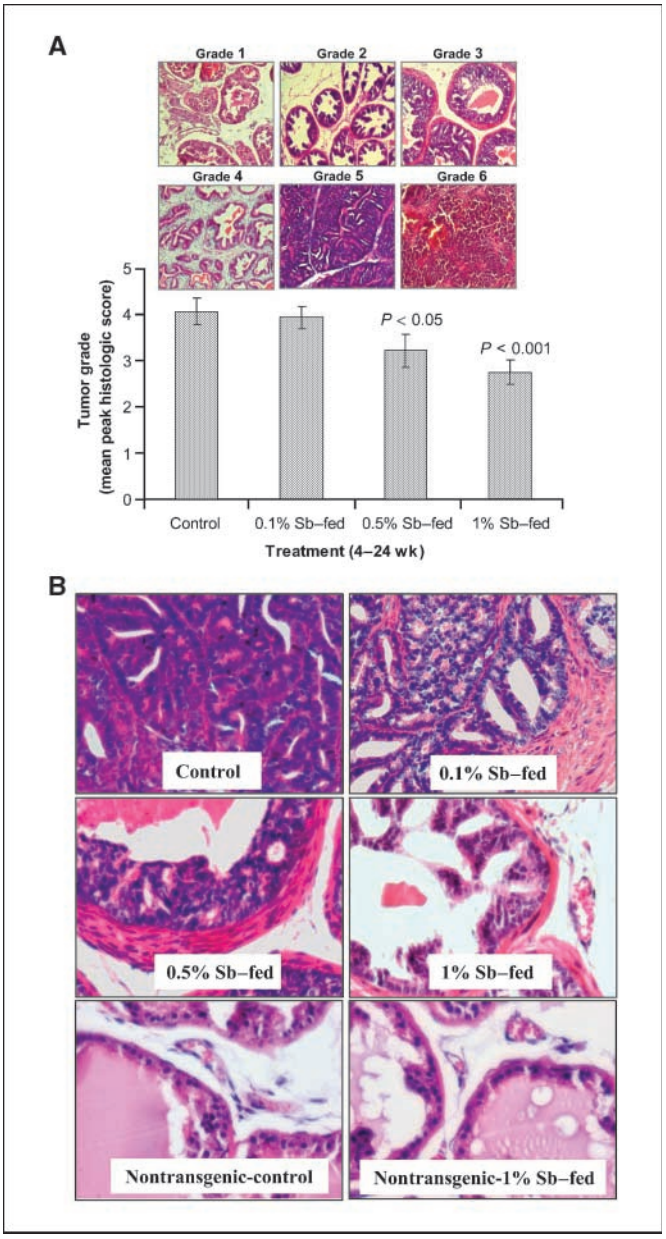

Figure 3. Silibinin feeding reduces the severity of prostatic lesions (tumor grade) of dorsolateral prostate in TRAMP/C57BL/6 mice. *A,* different stages of prostate tissues were graded as described in Results. The maximum histologic score for the prostate lobe was used to calculate the mean for the treatment group. *Columns,* mean peak histologic score of each group; *bars,* SE. The statistical significance of difference between positive control and silibinin-fed groups was analyzed by one-way ANOVA followed by Bonferroni *t* test for pairwise multiple comparisons. $P < 0.05$ was considered significant. *B,* the photomicrographs (×400 magnification) representative of the mean peak histologic score of a treatment group show the H&E staining of the dorsolateral prostate of positive control mice, silibinin-fed mice, and the nontransgenic mice fed either with control or 1% silibinin diet and sacrificed after 24 wk of age.

pathway during prostate tumor growth and progression in TRAMP/C57BL/6 mice. Immunohistochemical analysis of dorsolateral prostate tissue for IGF-IRβ showed both membrane and cytoplasmic staining (Fig. 5*A*). Silibinin-treated tissues showed more heterogeneous staining with patchy and focal patterns specifically in luminal cells compared with the positive control in which staining was heavy and more diffused (involving most areas of epithelium). Immunoreactivity scores for IGF-IRβ were 1.7 ± 0.3, 1.5 ± 0.3 ($P < 0.05$), and 1.5 ± 0.3 ($P < 0.05$) for 0.1%, 0.5% and 1% silibinin–fed groups of mice, respectively, compared with 2.9 ± 0.4 in the positive controls (Fig. 5*A*). These results were further confirmed by immunoblot analysis showing lower levels of IGF-IRβ protein in silibinin-fed groups (Fig. 5*A*). Densitometric analysis of bands (adjusted with β-actin as loading control) exhibited 58% to 63% ($P < 0.05$) decrease in IGF-IRβ protein expression in silibinin-fed groups of mice. Concomitant with decreased IGF-IRβ, dorsolateral prostate tissues from silibinin-fed groups of mice also showed reduced phosphorylation of IGF-IRβ at Tyr^{1131} in kinase domain compared with the positive controls (data not shown).

Regarding IGFBP-3, there was an increase in its cytoplasmic staining in silibinin-fed groups of mice compared with the positive controls (Fig. 5*B*). Immunoreactivity scores were 2.8 ± 0.3, 3.0 ± 0.2, and 3.6 ± 0.2 in 0.1%, 0.5%, and 1% silibinin–fed groups ($P < 0.001$, for all doses), respectively, compared with 1.2 ± 0.2 in the positive controls. Again, these findings were confirmed by immunoblot analysis of prostate tissue lysates, which showed higher IGFBP-3 levels in silibinin-fed groups (Fig. 5*B*). Densitometric analysis of bands (adjusted with β-actin as loading control)

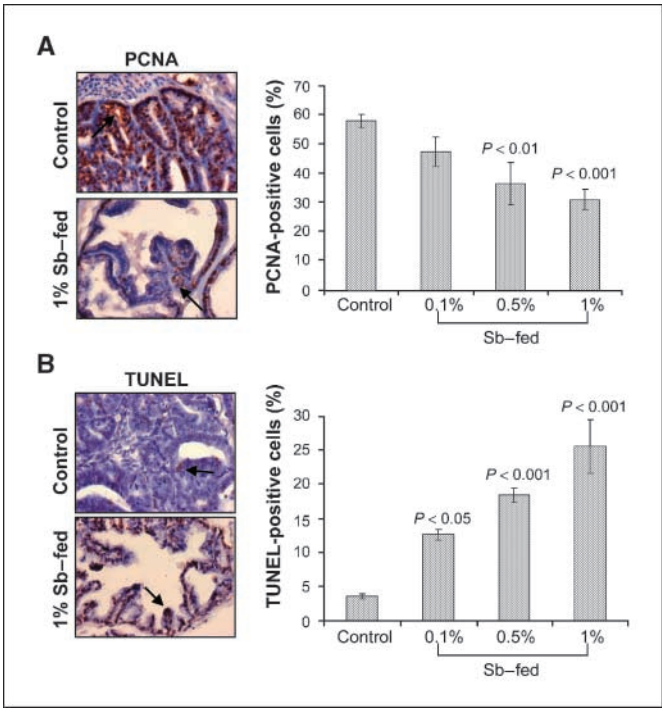

Figure 4. Antiproliferative and proapoptotic effects of dietary silibinin in TRAMP mice. *A, in vivo* antiproliferative effect of silibinin feeding on dorsolateral prostate of TRAMP/C57BL/6 mice. Immunohistochemical staining for PCNA in prostate was based on DAB staining as detailed in Materials and Methods. Representative DAB-stained tissue specimens from positive control and 1% silibinin–fed group (×400 magnifications). *Arrows,* PCNA-positive cells. *Columns,* mean PCNA-positive cells, quantified for determination of proliferation index in each group; *bars,* SE. *B, in vivo* proapoptotic effect of silibinin feeding on dorsolateral prostate in TRAMP/C57BL/6 mice. Apoptosis was analyzed by TUNEL staining in prostate tissues as detailed in Materials and Methods. Representative DAB-stained tissue specimens from positive control and 1% silibinin–fed group showing brown-colored TUNEL-positive cells are depicted at ×400 magnifications. *Arrows,* TUNEL-positive cells. Apoptotic index was calculated as the number of positive cells × 100 / total number of cells counted under ×400 magnifications in 10 randomly selected areas in each sample. *Bars,* SE. For both *A* and *B,* the statistical significance of difference between positive control and silibinin-fed groups was analyzed by one-way ANOVA followed by Bonferroni *t* test for pairwise multiple comparisons. $P < 0.05$ was considered significant.

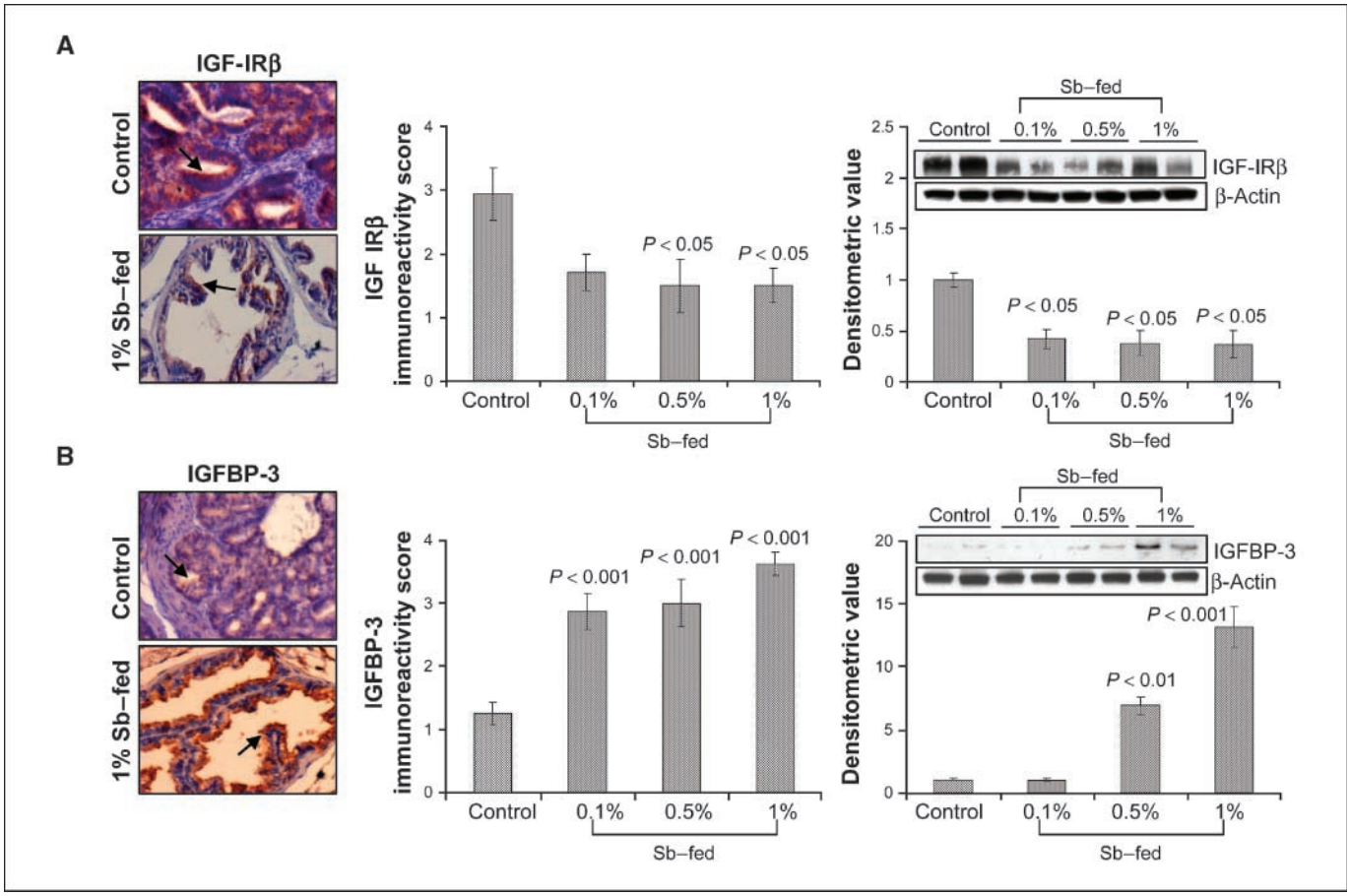

Figure 5. Effect of dietary feeding of silibinin on the expression of IGF-IRβ and IGFBP-3 in the dorsolateral prostate of TRAMP/C57BL/6 mice. Immunohistochemical staining/immunoblotting for IGF-IRβ (*A*) and IGFBP-3 (*B*) in prostate was done as detailed in Materials and Methods. Immunohistochemical staining was based on DAB staining as detailed in Materials and Methods. Representative DAB-stained tissue specimens from positive control and 1% silibinin–fed groups (×400 magnifications). *Arrows,* IGF-IRβ– and IGFBP-3–positive cells in the representative specimens. *Columns,* quantification of IGF-IRβ and IGFBP-3-positive cells represented as mean immunoreactivity score of each group; *bars,* SE. For both IGF-IRβ and IGFBP-3, immunoreactivity (represented by intensity of brown staining) was scored as 0 (no staining), +1 (nonuniform and very weak staining), +2 (nonuniform and weak staining), +3 (uniform and moderate staining), and +4 (uniform and strong staining). Randomly, prostate tissue samples of four individual mice were selected from each group for IGF-IRβ and IGFBP-3 immunoblotting. Reactive protein bands were visualized by enhanced chemiluminescence detection system, and membrane was stripped and reprobed with β-actin as loading control. *Columns,* mean densitometric values of band intensity, adjusted with β-actin, of the four bands from individual mouse prostate in each group; *bars,* SE. Representative blots of two prostate samples from each group. The statistical significance of difference between positive control and silibinin-fed groups was analyzed by one-way ANOVA followed by Bonferroni *t* test for pairwise multiple comparisons. $P < 0.05$ was considered significant.

showed ~7-fold ($P < 0.01$) and ~13-fold ($P < 0.001$) increase in IGFBP-3 levels in 0.5% and 1% silibinin–fed groups of mice, respectively, compared with the positive controls. In the first TRAMP/FVB experiment, serum levels of IGF-I, IGFBP-2, and IGFBP-3 were examined. Silibinin had no statistically significant effects on circulating levels of these hormones when compared with the positive control (data not shown). Together, these observations, for the first time, suggested that silibinin could inhibit the mitogenic action of IGF-I mostly via decreasing IGF-IRβ expression level and by an intratumoral up-regulation of IGFBP-3, which may also have IGF-I–independent activity during prostate tumor growth and progression in TRAMP model.

Silibinin modulates cell cycle regulators. We also determined the effect of silibinin feeding on the expression of cell cycle regulators in the prostate of TRAMP/C57BL/6 mice. Western blots for Cdks, cyclins, and Cdk inhibitors with densitometric data (adjusted with β-actin as loading control) are shown in Fig. 6. Here, it should be noted that membranes were stripped and reprobed for β-actin for each blot (data not shown). Silibinin strongly decreased protein levels of Cdk2, Cdk4, Cdk6, and Cdc2 by 73% to 97% ($P < 0.001$), 87% to 96% ($P < 0.001$), 91% to 97% ($P < 0.001$), and >99% ($P < 0.001$), respectively, in 0.1% to 1% silibinin–fed groups of mice compared with the positive controls (Fig. 6). Regarding protein levels of cyclins, 0.1%, 0.5%, and 1% silibinin showed a strikingly ~100% ($P < 0.001$, for all doses of silibinin) decrease in cyclin A; 22%, 39% ($P < 0.05$), and 75% ($P < 0.01$) decrease in cyclin B1; and 50%, 80% ($P < 0.05$), and 88% ($P < 0.01$) decrease in cyclin E, respectively (Fig. 6), without any effect on cyclin D1 and cyclin D3 (data not shown). Regarding Cdk inhibitors, there was a marked increase in the Cip1/p21 and Kip1/p27 protein levels in silibinin-fed groups (Fig. 6), which was significant with 0.5% and 1% doses, where ~4-fold ($P < 0.05$) and ~7-fold ($P < 0.05$) increases in Cip1/p21 and Kip1/p27 levels were observed for the two silibinin-fed groups of mice, respectively. Together, these results indicate that silibinin strongly decreases Cdks and cyclin expression with a concomitant increase in Cdk inhibitors to potentially inhibit cell cycle progression at G_1-S and G_2-M checkpoints, which could inhibit prostate tumor progression in TRAMP mice.

Discussion

The novel findings in the present study are that (*a*) oral silibinin, a common dietary supplement as well as a clinically used antihepatotoxic agent, inhibits prostate tumor growth and progression in TRAMP mice without any toxicity, and (*b*) the chemopreventive efficacy of silibinin is accompanied by the arrest of tumor progression at PIN stages with a concomitant decrease in adenocarcinoma, together with a decrease in cell proliferation and an increase in apoptotic cell death. Potential molecular mechanisms of silibinin efficacy, as identified in TRAMP model, are decreased expression of IGF-IRβ with a concomitant increase in cellular IGFBP-3 protein level and decreased expression of Cdks and cyclins with a concomitant increase in Cdk inhibitor (Cip1/p21 and Kip1/p27) protein levels.

In humans, progression of PCa is a multistage process involving the onset as a small carcinoma of low histologic grade progressing slowly to the metastatic lesions of higher grade. PCa development in TRAMP model closely mimics this human type of PCa progression in a stochastic fashion (20, 26). Chemopreventive strategies involving naturally occurring agents for PCa intervention are gaining increased attention because epidemiologic evidence suggests that dietary habits and lifestyle are among the major factors in PCa growth and progression (4–6, 27). In the last few decades, considerable progress has been made in this direction leading to identification of many cancer chemopreventive agents, one of them being silibinin, which has shown anticancer effects in various cancer cell types and animal tumor models (3, 9, 27–29).

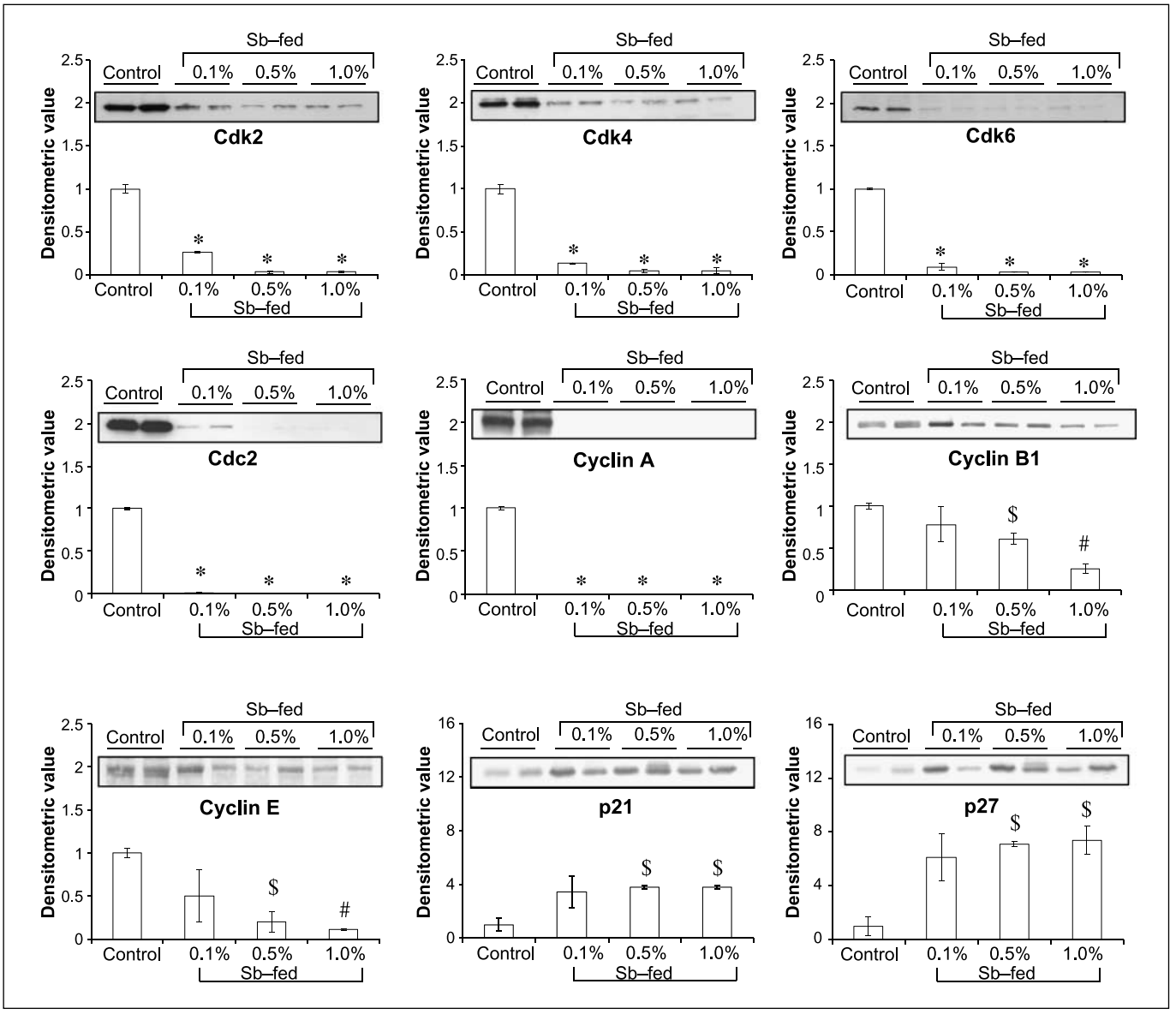

Figure 6. Silibinin feeding alters the expression levels of cell cycle regulatory molecules in the dorsolateral prostate of TRAMP/C57BL/6 mice. Randomly, four prostate tissue samples from individual mice were selected from each group for immunoblot analyses as detailed in Materials and Methods. Reactive protein bands for the expression of Cdk2, Cdk4, Cdk6, Cdc2, cyclin A, cyclin B1, cyclin E, Cip1/p21, and Kip1/p27 were visualized by enhanced chemiluminescence detection system, and membranes were stripped and probed with β-actin as loading control. *Columns,* mean densitometric values of band intensity for each protein, adjusted with β-actin (blots not shown), of the four bands from individual mouse prostate in each group; *bars,* SE. Representative blots of two prostate samples from each group are shown. The statistical significance of difference between positive control and silibinin-fed groups was analyzed by one-way ANOVA followed by Bonferroni *t* test for pairwise multiple comparisons. $P < 0.05$ was considered significant. *, $P < 0.001$; #, $P < 0.01$; $, $P < 0.05$.

In the present study, silibinin feeding reduced prostate adenocarcinoma incidence by slowing down tumor progression from PIN stages (premalignant) to adenocarcinoma (malignant), and this effect was independent of mouse strains as evidenced by similar trends in two different mouse strains (TRAMP/FVB and TRAMP/C57BL/6) used in the study. TRAMP mice from two different genetic backgrounds were studied because it has been reported that mice generated with C57BL/6 and FVB backgrounds show strain-specific responses to the transgene mediated transformation of the prostatic epithelium, and that the nature of progression is different in these two strains (16, 20). The TRAMP/C57BL/6 mice show a slower time to progression and live longer ($\sim$52 weeks), and they also display seminal vesicle invasion that can contribute disproportionately to the lower urogenital tract weight (20). The TRAMP/FVB mice show quick progression, develop large primary tumors, and rarely live beyond 32 weeks of age (20). By 30 weeks of age, TRAMP/FVB mice display 100% metastasis to lungs and lymph nodes along with bone metastasis, whereas TRAMP/C57BL/6 mice do not display 100% metastasis at this stage (20). In our present study, the anti–tumor progression effect of silibinin was observed to be dose dependent; additionally, in a similar fashion, it also reduced the severe form of adenocarcinoma (i.e., poorly/undifferentiated adenocarcinoma), which leads to a metastatic phenotype of the disease. The anti-PCa effect of silibinin was accompanied by a decrease in lower urogenital tract weight as well as antiproliferative and proapoptotic effects as observed by immunohistochemical analysis of prostate samples. Silibinin feeding did not negatively regulate the expression of transgene in prostate epithelial cells, which initiates the process of tumorigenesis. Further, silibinin feeding for 20 weeks starting from the 4th week of age neither showed any toxic effects in mice nor influenced normal histology of the prostate in nontransgenic mice, suggesting that silibinin could be an ideal chemopreventive agent to suppress prostate tumor growth and progression.

IGF-I signaling is reported to be deregulated in clinical PCa (30–33). Specifically, IGFBP-2 levels are often increased whereas those of IGFBP-3 are decreased, resulting in increased IGF-I levels (34–36). Furthermore, IGF-IR has been reported to be overexpressed in prostate tumor specimens (37). Silibinin feeding to TRAMP mice significantly reduced IGF-IR expression, as well as its activating tyrosine phosphorylation, and up-regulated IGFBP-3 protein levels. Because of high binding affinity of IGFBP-3 for IGF-I, these findings suggest that silibinin would have led to a lower amount of free IGF-I for its mitogenic action. We did not observe substantial changes in circulating IGF system in mouse serum from our first experiment (data not shown). The increase in tumor IGFBP-3 can prevent both systemic and local IGF effects on proliferation and survival. In addition, a strong increase in cellular IGFBP-3 may also exert antineoplastic effect through IGF-I–independent mechanisms, such as induction of apoptosis (38–40) as observed in the present study. This shows that silibinin acts specifically on tumor to increase IGFBP-3 and that it has insignificant effect on modulating the systemic IGF axis. This is a very "clean" effect without any disturbance in systemic IGF axis by silibinin treatment, which is different from some other agents such as somatostatin and lycopene that do affect systemic IGF axis (41, 42). Overall, pleiotropic molecular alterations were observed, suggesting down-regulation of IGF-I-IGF-IR–mediated signaling and an increase in cellular IGFBP-3 level by silibinin during inhibition of prostate tumor growth and progression. Because these modulations are implicated in both mitogenic and survival effects, as expected, silibinin also caused a marked decrease in cell proliferation and strongly enhanced apoptosis. Such *in vivo* effects of silibinin on these two biomarkers are also supported by our completed DU145 tumor xenograft study (14).

Further, based on our earlier *in vitro* studies in PCa cells (9), it was anticipated that the antiproliferative effect of silibinin against prostate tumor progression might also involve cell cycle regulatory mechanisms. The changing patterns of Cdks and cyclins have been well characterized during the progression of PCa in TRAMP model, wherein an up-regulation of mitotic cyclins, including cyclin A, cyclin B, and cyclin E, and a decrease in cyclin D1 have been observed (43). The levels of cyclin D3 showing increased expression compared with normal prostate do not greatly vary during the disease progression (43). In our present study, silibinin down-regulated the expression of Cdk2, Cdk4, Cdk6, and Cdc2, as well as cyclin E, cyclin A, and cyclin B1, in the prostate of TRAMP mice. Additionally, silibinin also increased the protein expression of Cdk inhibitors, Cip1/p21 and Kip1/p27, which are well known to interact with and inhibit kinase activity of Cdk-cyclin complex (3). Therefore, the anti–tumor progression effect of silibinin in TRAMP mice could most likely be mediated, at least in part, via its effect on Cdk-cyclin-Cdk inhibitor axis.

In summary, silibinin feeding inhibits prostate tumor growth as well as progression in TRAMP mice without any adverse health effects. Potential mechanisms for this anti-PCa effect of silibinin are most likely the down-modulation of IGF-I signaling and decrease in Cdk-cyclin kinase activity leading to an inhibition of cell cycle progression accompanied by decreased cell proliferation and enhanced apoptosis. These findings, together with those in nude mice DU145 xenograft, suggest that silibinin could be a useful agent for PCa prevention and intervention. Finally, we would like to mention that based on our extensive preclinical studies with silibinin in PCa models, we have successfully completed a National Cancer Institute–funded phase I clinical trial in human PCa patients (44) and are currently conducting a pilot phase II clinical trial. In this regard, present findings on the anti–tumor progression effect of silibinin with potential molecular mechanisms would have paramount significance.

References

1. Stewart AB, Lwaleed BA, Douglas DA, Birch BR. Current drug therapy for prostate cancer: an overview. Curr Med Chem Anti-Canc Agents 2005;5:603–12.
2. Agarwal R. Cell signaling and regulators of cell cycle as molecular targets for prostate cancer prevention by dietary agents. Biochem Pharmacol 2000; 60:1051–9.
3. Singh RP, Agarwal R. Mechanisms of action of novel agents for prostate cancer chemoprevention. Endocr Relat Cancer 2006;13:751–78.
4. Kelloff GJ, Sigman CC, Greenwald P. Cancer chemoprevention: progress and promise. Eur J Cancer 1999;35: 2031–8.

5. Thompson IM, Tangen CM, Klein EA, Lippman SM. Phase III prostate cancer prevention trials: are the costs justified? J Clin Oncol 2005;23:8161–4.

6. Shukla S, Gupta S. Dietary agents in the chemoprevention of prostate cancer. Nutr Cancer 2005;53:18–32.

7. Kaur M, Agarwal R. Silymarin and epithelial cancer chemoprevention: how close we are to bedside? Toxicol Appl Pharmacol; Advance Access published online Nov 15th 2006.

8. Wellington K, Jarvis B. Silymarin: a review of its clinical properties in the management of hepatic disorders. BioDrugs 2001;15:465–89.

9. Singh RP, Agarwal R. Prostate cancer chemoprevention by silibinin: bench to bedside. Mol Carcinog 2006; 45:436–42.

10. Zi X, Grasso AW, Kung HJ, Agarwal R. A flavonoid antioxidant, silymarin, inhibits activation of erbB1 signaling and induces cyclin-dependent kinase inhibitors, G_1 arrest, and anticarcinogenic effects in human prostate carcinoma DU145 cells. Cancer Res 1998;58: 1920–9.

11. Zi X, Agarwal R. Silibinin decreases prostate-specific antigen with cell growth inhibition via G_1 arrest, leading to differentiation of prostate carcinoma cells: implications for prostate cancer intervention. Proc Natl Acad Sci U S A 1999;96:7490–5.

12. Zi X, Zhang J, Agarwal R, Pollak M. Silibinin upregulates insulin-like growth factor-binding protein 3 expression and inhibits proliferation of androgen-independent prostate cancer cells. Cancer Res 2000;60: 5617–20.

13. Deep G, Singh RP, Agarwal C, Kroll DJ, Agarwal R. Silymarin and silibinin cause G_1 and G_2-M cell cycle arrest via distinct circuitries in human prostate cancer PC3 cells: a comparison of flavanone silibinin with flavanolignan mixture silymarin. Oncogene 2006;25: 1053–69.

14. Singh RP, Dhanalakshmi S, Tyagi AK, Chan DC, Agarwal C, Agarwal R. Dietary feeding of silibinin inhibits advance human prostate carcinoma growth in athymic nude mice and increases plasma insulin-like growth factor-binding protein-3 levels. Cancer Res 2002; 62:3063–9.

15. Gingrich JR, Greenberg NM. A transgenic mouse prostate cancer model. Toxicol Pathol 1996;24:502–4.

16. Greenberg NM, DeMayo F, Finegold MJ, et al. Prostate cancer in a transgenic mouse. Proc Natl Acad Sci U S A 1995;92:3439–43.

17. Greenberg NM, DeMayo FJ, Sheppard PC, et al. The rat probasin gene promoter directs hormonally and developmentally regulated expression of a heterologous gene specifically to the prostate in transgenic mice. Mol Endocrinol 1994;8:230–9.

18. Gingrich JR, Barrios RJ, Kattan MW, Nahm HS, Finegold MJ, Greenberg NM. Androgen-independent prostate cancer progression in the TRAMP model. Cancer Res 1997;57:4687–91.

19. Gingrich JR, Barrios RJ, Morton RA, et al. Metastatic prostate cancer in a transgenic mouse. Cancer Res 1996; 56:4096–102.

20. Kaplan-Lefko PJ, Chen TM, Ittmann MM, et al. Pathobiology of autochthonous prostate cancer in a pre-clinical transgenic mouse model. Prostate 2003;55: 219–37.

21. Zhao J, Agarwal R. Tissue distribution of silibinin, the major active constituent of silymarin, in mice and its association with enhancement of phase II enzymes: implications in cancer chemoprevention. Carcinogenesis 1999;20:2101–8.

22. Singh RP, Sharma G, Dhanalakshmi S, Agarwal C, Agarwal R. Suppression of advanced human prostate tumor growth in athymic mice by silibinin feeding is associated with reduced cell proliferation, increased apoptosis, and inhibition of angiogenesis. Cancer Epidemiol Biomarkers Prev 2003;12:933–9.

23. Hwang DL, Lee PD, Cohen P. Quantitative ontogeny of murine insulin-like growth factor (IGF)-I, IGF-binding protein-3 and the IGF-related acid-labile subunit. Growth Horm IGF Res. Epub 2007 Aug 22.

24. Shappell SB, Thomas GV, Roberts RL, et al. Prostate pathology of genetically engineered mice: definitions and classification. The consensus report from the Bar Harbor meeting of the Mouse Models of Human Cancer Consortium Prostate Pathology Committee. Cancer Res 2004;64:2270–305.

25. Hurwitz AA, Foster BA, Kwon ED, et al. Combination immunotherapy of primary prostate cancer in a transgenic mouse model using CTLA-4 blockade. Cancer Res 2000;60:2444–8.

26. Gingrich JR, Barrios RJ, Foster BA, Greenberg NM. Pathologic progression of autochthonous prostate cancer in the TRAMP model. Prostate Cancer Prostatic Dis 1999;2:70–5.

27. Bidoli E, Talamini R, Bosetti C, et al. Macronutrients, fatty acids, cholesterol and prostate cancer risk. Ann Oncol 2005;16:152–7.

28. Singh RP, Agarwal R. A cancer chemopreventive agent silibinin, targets mitogenic and survival signaling in prostate cancer. Mutat Res 2004;555:21–32.

29. Singh RP, Agarwal R. Prostate cancer prevention by silibinin. Curr Cancer Drug Targets 2004;4:1–11.

30. Chan JM, Stampfer MJ, Giovannucci E, et al. Plasma insulin-like growth factor-I and prostate cancer risk: a prospective study. Science 1998;279:563–6.

31. Cohen P. Serum insulin-like growth factor-I levels and prostate cancer risk-interpreting the evidence. J Natl Cancer Inst 1998;90:876–9.

32. Pollak MN. Insulin-like growth factors and prostate cancer. Epidemiol Rev 2001;23:59–66.

33. Pollak MN, Schernhammer ES, Hankinson SE. Insulin-like growth factors and neoplasia. Nat Rev Cancer 2004;4:505–18.

34. Tennant MK, Thrasher JB, Twomey PA, Birnbaum RS, Plymate SR. Insulin-like growth factor-binding protein-2 and -3 expression in benign human prostate epithelium, prostate intraepithelial neoplasia, and adenocarcinoma of the prostate. J Clin Endocrinol Metab 1996;81:411–20.

35. Cohen P, Peehl DM, Stamey TA, Wilson KF, Clemmons DR, Rosenfeld RG. Elevated levels of insulin-like growth factor-binding protein-2 in the serum of prostate cancer patients. J Clin Endocrinol Metab 1993;76:1031–5.

36. Kanety H, Madjar Y, Dagan Y, et al. Serum insulin-like growth factor-binding protein-2 (IGFBP-2) is increased and IGFBP-3 is decreased in patients with prostate cancer: correlation with serum prostate-specific antigen. J Clin Endocrinol Metab 1993;77:229–33.

37. Liao Y, Abel U, Grobholz R, et al. Up-regulation of insulin-like growth factor axis components in human primary prostate cancer correlates with tumor grade. Hum Pathol 2005;36:1186–96.

38. Rajah R, Valentinis B, Cohen P. Insulin-like growth factor (IGF)-binding protein-3 induces apoptosis and mediates the effects of transforming growth factor-β1 on programmed cell death through a p53- and IGF-independent mechanism. J Biol Chem 1997;272:12181–8.

39. Cobb LJ, Liu B, Lee KW, Cohen P. Phosphorylation by DNA-dependent protein kinase is critical for apoptosis induction by insulin-like growth factor binding protein-3. Cancer Res 2006;66:10878–84.

40. Bhattacharyya N, Pechhold K, Shahjee H, at al. Nonsecreted insulin-like growth factor binding protein-3 (IGFBP-3) can induce apoptosis in human prostate cancer cells by IGF-independent mechanisms without being concentrated in the nucleus. J Biol Chem 2006;281: 24588–601.

41. Spranger J, Buhnen J, Jansen V, et al. Systemic levels contribute significantly to increased intraocular IGF-I, IGF-II and IGF-BP3 in proliferative diabetic retinopathy. Horm Metab Res 2000;32:196–200.

42. Graydon R, Gilchrist SE, Young IS, Obermuller-Jevic U, Hasselwander O, Woodside JV. Effect of lycopene supplementation on insulin-like growth factor-1 and insulin-like growth factor binding protein-3: a double-blind, placebo-controlled trial. Eur J Clin Nutr. Epub ahead of print 2007 Feb 7.

43. Maddison LA, Huss WJ, Barrios RM, Greenberg NM. Differential expression of cell cycle regulatory molecules and evidence for a "cyclin switch" during progression of prostate cancer. Prostate 2004;58:335–44.

44. Flaig TW, Gustafson DL, Su LJ, et al. A phase I pharmacokinetic study of silybin-phytosome in prostate cancer patients. Invest New Drugs 2007;25:139–46.